Smart Structures and Systems, *Vol. 33, No. 3 (2024) 243-251*
https://doi.org/10.12989/sss.2024.33.3.243

Modeling of vibration protection by shape memory alloy parts with an account of latent heat

Fedor S. Belyaev [1,2a], Margarita E. Evard[*2], Aleksandr E. Volkov [2b] and Maria S. Starodubova [2c]

[1] *Laboratory of Mathematical Methods in Mechanics of Materials, Institute for Problems in Mechanical Engineering of the RAS, V.O., Bolshoj pr. 61, St. Petersburg, 199178, Russia*
[2] *Saint Petersburg State University, Universitetskaya Nab. 7-9, St. Petersburg, 199034, Russia*

(*Received July 27, 2023, Revised January 18, 2024, Accepted February 10, 2024*)

Abstract. Modeling of vibrations of a rotating pendulum with working shape memory alloy rod has been performed in the frames of a microstructural model taking into account the latent heat release, absorption and the heat exchange during direct and reverse martensitic transformation. It has been shown that the influence of the latent heat, the rate of preliminary deviation of the pendulum from the equilibrium, the rate of heating and cooling can have a significant impact on the vibrations and damping characteristics of the system.

Keywords: damping; heat exchange conditions; latent heat; microstructural modeling; shape memory alloys; TiNi; vibration protection

1. Introduction

Due to their high damping ability, shape memory alloys (SMA) have been under consideration as working elements of various dampers since 1990s (Casciati *et al*. 1998). Furthermore, SMA, being the functional materials with different stiffness at different temperatures, have found their niche in the field of vibration protection and control (Casciati 2019, Torra *et al*. 2015).

In the case of passive vibration control, the use of SMA is advantageous due to the non-linear stress-strain characteristic and the mechanical hysteresis providing high damping ability. The control is carried out by selecting the composition of the alloy that provides the required characteristics of the SMA in a specific operating temperature range. (Khan *et al*. 2004, Lagoudas *et al*. 2004, Tiwari *et al*. 2021). Small variations of the chemical composition of an SMA allow shifting temperatures of the martensitic transformation so that the SMA element at the operation temperature can be in the austenitic, martensitic or two-phase state. When used in the damping devices, austenitic SMA parts undergoing the direct martensitic transformation and demonstrating the pseudoelasticity can accumulate a large unelastic deformation at a small hardening rate (Kaup *et al*. 2021). This deformation is reversible on unloading and leads to the recovery of the initial position of the structure after the cease of vibrations. Therefore, pseudoelastic parts are good in the cases when the so-called re-centering ability is crucial. However, the energy dissipation is much higher if the SMA is in the martensitic state when the unelastic deformation mechanism is the re-orientation of martensitic domains (Casciati *et al*. 1998). For seismic applications the low level of the yield stress can be important. In SMA it strongly depends on the temperature and is very low for the two-phase state of the alloy. In the case of using an SMA the control factor is the temperature variation, which can cause reversible martensitic transformations and thus change the mechanical properties of an alloy.

The semi-active and active vibration control by SMA-based devices is realized by heating or cooling of an SMA part. The variation of stiffness due to the phase transformation causes the change of the cutoff and resonance frequencies of vibrating systems, which permits to control the vibration regime, escape from the resonance and to switch between the vibroisolation and damping modes of vibration protection (Volkov *et al*. 2013, 2014). This way of control is usually referred to as the semi-active one. For the active control a programmed mode of temperature variations with heating or cooling in certain moments of oscillations can be used. On heating an SMA part undergoes the reverse martensitic transformation generating a stress opposite to the preliminary deformation, while on cooling the direct transformation causes the relaxation of the existing stress. In the works (Belyaev and Volkov 2001, Belyaev *et al*. 1999, 2003) it was shown that if heating and cooling are fast enough, temperature variations can be organized in a way to intensify the vibration, to keep it sustained or to provide its rapid decay. Therefore, the use of SMA elements has opened the ways to combine passive damping and active vibration control. In the review of 2022 (Tabrizikahou *et al*. 2022) the authors

*Corresponding author, Ph.D., Associate Professor,
E-mail: m.evard@spbu.ru
[a] Ph.D., Senior Researcher
[b] D.Sci. Professor
[c] Ph.D. Student

ISSN: 1738-1584 (Print), 1738-1991 (Online)

both traced the historical development of different engineering applications and introduced novel structural response control methods in SMA seismic applications.

A numerical simulation of a SMA vibration protection may be definitely helpful for developing practical applications because it gives an opportunity to make a quick test of the applicability of a specific SMA and to predict the level of vibrations in particular conditions. For modeling of SMA elements different theoretical approaches can be used. For isothermal deformation and simple stress-strain states possibly most appropriate are well-known phenomenological models (Tanaka and Iwasaki 1985, Boyd and Lagoudas 1996, Liang and Rogers 1990, Pence 1999) or models of an interpolation type (Trochu and Terriault 1998). The authors of the review of SMA applications for vibration control (Tabrizikahou *et al*. 2022) referred to the models of Graesser and Cozzarelli (Graesser and Cozzarelli 1991), Wilde, Gardoni and Fujino (Wilde *et al*. 2000) and Tanaka (Tanaka *et al*. 1995) as the most frequently utilized one-dimensional SMA material models for seismic design purposes. However, a shape memory element used as a working material for a vibration protection device is subject to a rather complicated thermomechanical loading, usually neither stress nor temperature is constant. That is why microstructural models accounting for mechanisms and physical laws of deformations are more reliable than macro-mechanical models or models using isobaric or isothermal interpolation of stress-strain, stress-temperature or strain temperature curves. Among such models are those of E. Patoor (Patoor *et al*. 1996), Q.-P. Sun and C. Lexcellent (Sun and Lexcellent 1996), X. Gao, M. Huang and C. Brinson (Gao *et al*. 2000, Huang *et al*. 2000) and others. The microstructural approach described in Likhachev (1995) and further developed in Evard and Volkov (1999), Belyaev *et al*. (2019, 2022) was successfully used for modeling of different vibration protection devices (Belyaev and Volkov 2001, Belyaev *et al*. 1999, 2003, Volkov *et al*. 2013, 2014). But all the calculations did not take into account the release and absorption of the latent heat during the martensitic transformations. Meanwhile, this effect may significantly increase the temperature of an SMA part and substantially change its behavior (Pieczyska *et al*. 2013, Kato 2021, Louia *et al*. 2023). Experimental investigations on NiTi have shown that the material temperature oscillates due to latent-heat release/absorption during cyclic loading. Moreover, the oscillation amplitude increases with the loading rate and can eventually reach a saturation value (He and Sun 2010, Yin *et al*. 2014). Such temperature variations during cyclic loading may significantly affect the functional properties and the fatigue life of the material. Of course, the modification of the temperature could be attenuated by dissipating the heat through heat exchange with the surrounding medium (Leo *et al*. 1993, McCormick *et al*. 1993), but sometimes the heat exchange may be impeded, especially when an SMA element has some coating (Qiu *et al*. 2020, Jin *et al*. 2024) or is additively manufactured (Yan *et al*. 2023).

When someone tries to take into account the latent heat release and absorption in modeling they usually have to use the phenomenological models of SMA mechanical behavior. Such a fully coupled thermo-mechanical constitutive macroscopic model for SMA taking into account latent heat effects during forward and reverse martensitic phase transformations was solved in the work (Armattoe *et al*. 2016). The authors described a delaying effect of the transformation latent heat on the forward and reverse phase transformations in SMA even in thin structures. In the work (Helbert *et al*. 2020) a macro-mechanical model based on two yield surfaces (Helbert *et al*. 2017) was used for modeling of a vibrating beam under free oscillations for axial and transversal vibrations.

In the present work, an attempt is made to simulate control of vibrations with SMA parts taking into account the latent heat and the heat exchange conditions by means of the microstructural model (Belyaev *et al*. 2019), a brief description of which is given in the next item. This model was previously tested on simulation of various effects in SMAs, including cyclic behavior in different phase states, accumulation of irreversible micro-plastic deformation, fatigue deterioration and so on. But in this article the emphasis is made on studying the influence of latent heat on vibrations, so these effects have not been taken into account.

2. Model

The representative volume consists of grains characterized by orientations of the crystallographic axes. Inside each of the grains austenite and martensite can coexist. Martensite is composed of domains originated by one of N crystallographically equivalent Bain's lattice deformations. Reuss' scheme is used for calculation of the strain tensor for the representative volume by the neutralization of the strains of grains belonging to this volume. Small strain tensors are used. The strain of each grain ε^{gr} is calculated as the sum of micro-strains delivered by various deformation mechanisms: elastic ε^{e}, thermal expansion ε^{T} and phase transformation ε^{Ph}

$$\varepsilon^{gr} = \varepsilon^{e} + \varepsilon^{T} + \varepsilon^{Ph}. \tag{1}$$

The main goal of the present work is to estimate the effect of the latent heat. So, for simplicity, the terms describing strains corresponding to accommodation plasticity and active plastic deformation were not included in (1), even though the microstructural model has such means (for example, Belyaev *et al*. 2022). Besides, note that in many applications the design envisages a relatively low level of stresses, when plastic deformation of the SMA part can be neglected.

Elastic and thermal strains are found for austenite and martensite in the common way by the Hook's law and the law of thermal expansion. The "mixture rule" is used to find these strains when two phases coexist. The phase deformation ε^{Ph} of a single martensite variant equals to the Bain's deformation D_n. The phase deformation of a grain on the whole is the average over the martensite variants

$$\varepsilon^{Ph} = \frac{1}{N}\sum_{n=1}^{N} \Phi_n D^n, \tag{2}$$

where Φ_n are such internal variables that Φ_n/N is the volume fraction of the n-th Bain's variant of martensite in the grain. The total volume fraction of martensite Φ^{gr} in a grain and the phase strain of the grain ε^{Ph} are calculated as

$$\Phi^{gr} = \frac{1}{N}\sum_{n=1}^{N} \Phi_n. \tag{3}$$

It is supposed that spatial averaging can be replaced by orientation averaging, so that the strain of the representative volume is calculated by the sum of the strains $\varepsilon^{gr}(\omega)$ of the grains

$$\varepsilon = \sum_{\omega} f(\omega)\varepsilon^{gr}(\omega), \tag{4}$$

where $f(\omega)$ is the volume fraction of grains with orientation ω.

Thermodynamic forces determining the evolution of the internal variables Φ_n are obtained as derivatives of the Gibbs' potential G. For a unit volume of the two-phase material it can be split into the eigen potential G^{eig} and the potential of mixing G^{mix}

$$G = G^{eig} + G^{mix}. \tag{5}$$

The eigen potential is the potential of non-interacting austenite and martensite and is calculated by relations given, for example, in the work (Volkov and Casciati 2001)

$$G^{eig} = (1-\Phi^{gr})G^{A} + \frac{1}{N}\sum_{n=1}^{N} \Phi_n G^{Mn}, \tag{6}$$

$$G^{a} = G_0^a - S_0^a(T-T_0) - \frac{c_\sigma^{0a}(T-T_0)^2}{2T_0} - \varepsilon_{ij}^{0Ta}(T)\sigma_{ij} - \frac{1}{2}Q_{ijkl}^{a}\sigma_{ij}\sigma_{kl}, \quad a = A, Mn, \tag{7}$$

where T_0 is the temperature of the thermodynamic equilibrium of austenite and martensite at zero stress, G_0^a and S_0^a are the values of the Gibbs' potential and of the entropy at $T = T_0$ and $\sigma_{ij} = 0$, c_σ^a is the specific heat (per unit volume), $\varepsilon_{ij}^{0a}(T)$ is the strain at $\sigma_{ij} = 0$, Q^a_{ijkl} is the tensor of elastic compliances.

The potential of mixing G^{mix} corresponds to the elastic energy of the internal stresses caused by the incompatibilities of the phase deformation. In this work we use the simplest quadratic form for G^{mix}

$$G^{mix} = \frac{\mu}{2}\sum_{m,n=1}^{N} A_{mn}\Phi_m\Phi_n. \tag{8}$$

Here material constants μ and A_{mn} describe the magnitude of the interaction as well as the preference of the appearance of the particular combinations of the martensite Bain's variants. An estimation of the values of these constants for TiNi was considered in Volkov *et al*. (2015). The condition of the transformation is formulated in terms of the generalized thermodynamic forces. From Eqs. (5)-(8) the thermodynamic forces for the martensitic transformation are derived as

$$F_n = -\frac{\partial G}{\partial \Phi_n} \approx \frac{q_0(T-T_0)}{T_0} + D_{ij}^n\sigma_{ij} - \mu\sum_{m=1}^{N} A_{mn}\Phi_m, \tag{9}$$

where q_0 is latent heat of the direct martensitic transformation.

Since a temperature-phase hysteresis exists, one concludes that the transformation occurs in conditions apart from the equilibrium. Thus, we formulate the condition of the transformation in the form

$$F_n = \pm F^{fr}, \tag{10}$$

where F^{fr} is the "friction force", which acts similarly to a dry friction force and is responsible for the temperature-phase hysteresis, sign "+" is taken for the direct and "–" for the reverse transformation. Constants F^{fr} and μ are related to the characteristic temperatures and the latent heat of the transformation. From this condition one can establish the procedure to evaluate the internal parameters $\Phi_n(\omega)$.

A special approach to describe the reorientation (twinning) of martensite is described in Volkov *et al*. (2014). Note that reorientation is not accompanied by the heat release/absorption.

3. Modelling

3.1 Model of a vibrating system

Following (Belyaev and Volkov 2001, Belyaev *et al*. 2003) to simulate vibrational control with the use of a SMA element, we consider a model of a rotation pendulum (Fig. 1). The pendulum consists of a beam of length $2L$ with two masses m on each its end. The beam is attached to an SMA rod with length l and diameter d. Linear stress dependence on the radius is assumed.

It should be noted that the boundary value problem was not solved here. Since these are the outer layers of the rod that give the main contribution into producing of the torque, the tangential stress and the shear strain are referred to this layer and the maximum stress value was used for calculation of the SMA strain response.

Theoretical model of a SMA described above provides the possibility of calculating the increment of the SMA strain for given increments of temperature and stress, thus

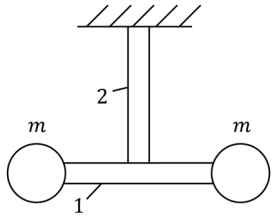

Fig. 1 Model of the rotation pendulum

1 – beam with two attached masses m
2 – SMA rod

representing the constitutive law. The system of ordinary differential equations describing rotation of the pendulum, which allow obtaining increments of the stress, the angle of rotation and the internal variables of the model were presented in details in the work (Belyaev and Volkov 2001).

The model has shown good correspondence with available experimental results of torsion tests on SMA bars (Meisner and Sivokha 2004, Song *et al*. 2019).

3.2 Thermal balance and parameters of the system

A TiNi-type alloy was chosen as a model material for the SMA part. Suggesting for the simplicity that the temperature distribution in the SMA rod is uniform and the heat exchange occurs from its surface in accordance with Newton's convection law, one can write the heat balance equation

$$-\left(\rho_M \Phi_M + \rho_A(1-\Phi_M)\right)\left(C_M \Phi_M + C_A(1-\Phi_M)\right)\dot{T} + h_{conv}\frac{A_{SMA}}{V_{SMA}}(T_{amb}-T) = q_0 \dot{\Phi}_M, \quad (11)$$

where ρ_M and ρ_A are the densities of martensite and austenite, C_M and C_A are the specific heats of martensite and austenite, Φ_M is the total volume fracture of martensite, T_{amb} is the ambient temperature, h_{conv} is the heat transfer coefficient, A_{SMA} and V_{SMA} are the area and volume of the TiNi rod, dot means the time derivative. The values of h_{conv} were chosen as 0 (corresponds to an adiabatic process), 10 (corresponds to a metal-air heat exchange), 500 (a metal-water heat exchange) and 5000 W/(m^2 K) (a metal-water heat exchange at forced convection). Although cooling by water can often be difficult, there exist quite a few application designs using the liquid cooling, for example Wang *et al*. (2008), Tadesse *et al*. (2010), Regany *et al*. (2022).

Material constants for SMA and characteristics of the vibrating system are presented in the Table 1.

Table 1 Parameters for TiNi element and vibrating system

Material constant	Symbol	Value
Number of martensite variants	N	12
Latent heat of the direct martensitic transformation	q_0	-160 MJ/m^3
Characteristic temperatures	Mf Ms As Af	324 K 333 K 351 K 360 K
Density of martensite	ρ_M	6.5×10^3 kg/m^3
Density of austenite	ρ_A	6.5×10^3 kg/m^3
Specific heat of martensite	C_M	500 J/(kg×K)
Specific heat of austenite	C_A	550 J/(kg×K)
Shear modulus of martensite	G_M	12 GPa
Shear modulus of austenite	G_A	30 GPa
Parameters of the pendulum		
Beam length	L	2 m
Masses	m	40 kg
Length of the SMA rod	l	200 mm
Diameter of the SMA rod	d	22 mm

3.3 Results of simulation

Fig. 2 illustrates the influence of the heat exchange conditions on the stress-strain diagrams at free vibration at constant ambient temperature T_{amb} = 360 K when the SMA rod is in the austenitic pseudoelastic state and on loading and unloading experiences reversible transformations. The initial angular deviation of the pendulum from the equilibrium corresponds to the shear strain of 8.25%, which is achieved during 100 s (further, we will refer to this process as the slow deformation). One can see that the adiabatic stress-strain loop is narrower than the isothermal

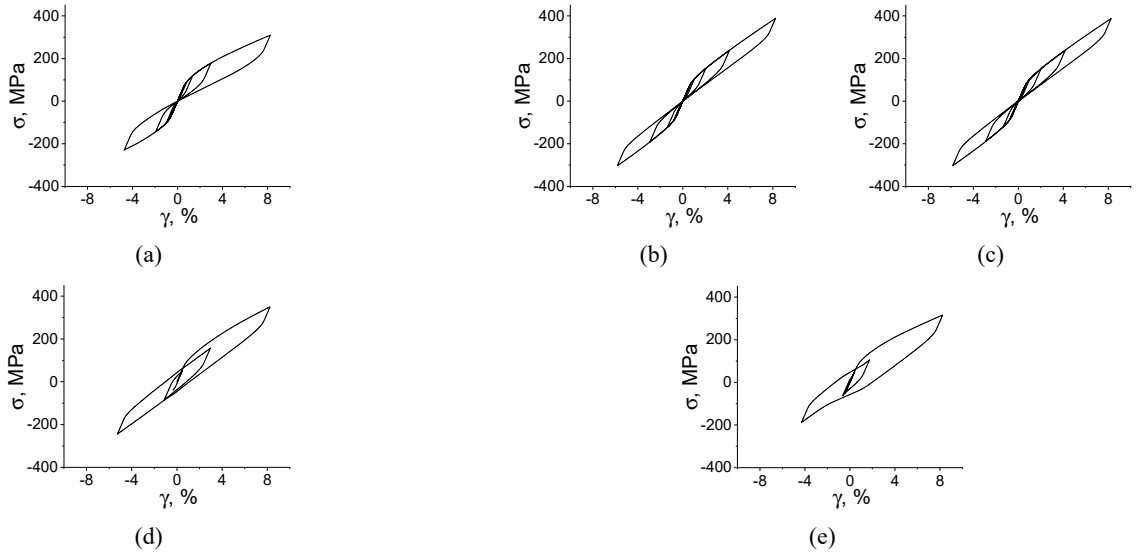

Fig. 2 Tangential stress – shear diagrams of the SMA element at the ambient temperature 360 K corresponding to (a) isothermal deformation; (b) adiabatic deformation; (c) heat exchange with $h_{conv} = 10$ W/(m^{2}K); (d) $h_{conv} = 500$ W/(m^{2}K); (e) $h_{conv} = 5000$ W/(m^{2}K)

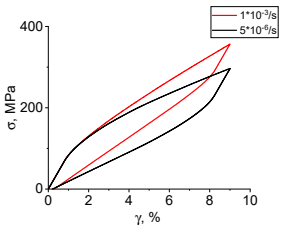

Fig. 3 Tangential stress – shear diagram of the SMA element at the ambient temperature 360 K at different strain rates

one and the loop in case of the metal-air heat exchange is similar to the adiabatic one. The stress-strain loops for the heat exchange with water are wider and one can expect more effective damping of vibrations in comparison with other cases.

To verify the obtained results, modeling of stress-strain diagrams at different shear rates were performed. Fig. 3 illustrates the diagrams calculated at the temperature 360 K. The strain rate $5 * 10^{-6}/s$ corresponds to the near-isothermal regime; the maximal temperature variation was less than 1 K. At the strain rate $1 * 10^{-3}/s$, corresponding to near-adiabatic regime, the maximal temperature variation was about 20 K. These results are in good qualitative agreement with the experimental data of Kan *et al*. (2016).

The vibrograms and the corresponding temperature variation profiles are presented on Fig. 4. During initial deformation the growth of the SMA rod temperature is about 17 K for the adiabatic (4b) and air-cooling (4c) cases, 10 K for the water-cooling case (4d) and 0 K for the water-cooling with forced convection case (4e). Following vibrations provoke heat absorption/release and change the vibrograms in comparison with the isothermal case. Influence of heat absorption is most appreciable for the

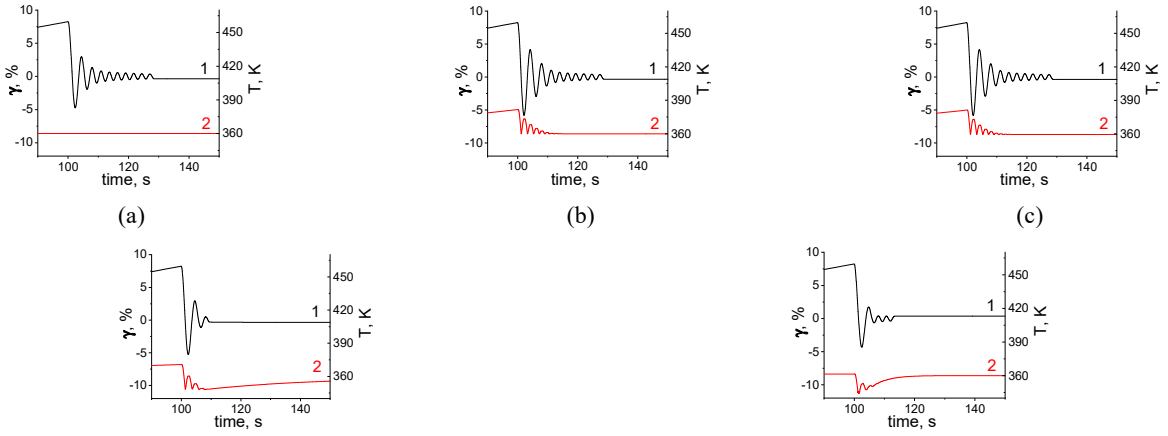

Fig. 4 Dependence of shear strain γ (1) and temperature T(2) on time on time with the ambient temperature 360 K corresponding to (a) isothermal deformation; (b) adiabatic deformation; (c) heat exchange with $h_{conv} = 10$ W/(m^{2}K); (d) $h_{conv} = 500$ W/(m^{2}K); (e) $h_{conv} = 5000$ W/(m^2 K)

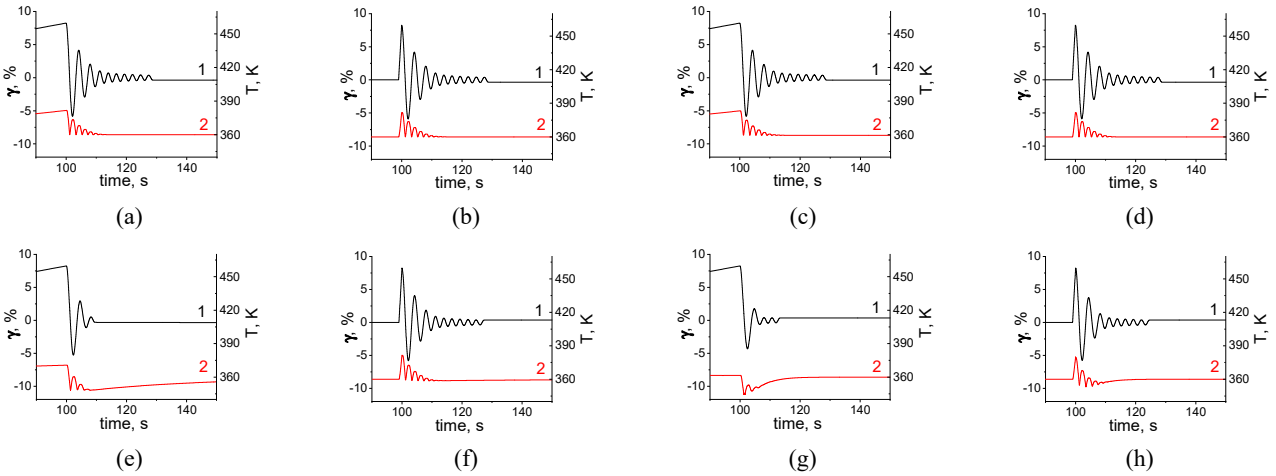

Fig. 5 Dependence of shear strain γ(1) and temperature T(2) on time with the ambient temperature 360 K; (a), (b) – adiabatic regime; (c), (d) – heat exchange with $h_{conv} = 10$ W/(m^{2}K); (e), (f) – heat exchange with $h_{conv} = 500$ W/(m^{2}K); (g), (h) – heat exchange with $h_{conv} = 5000$ W/(m^{2}K);
(a), (c), (e), (g) – slow initial deformation; (b), (d), (f), (h) – fast initial deformation

water-cooling cases. The temperature decreases to 350 K for the free water convection (4d) and to 345 K for the forced convection (4e). This "natural" cooling causes increase of the martensitic phase and rapid decay of vibrations.

Besides the slow initial deformation and following free vibration, the regime of the fast initial deformation to the same value of the shear strain (8.25%) during 1 s was considered. The results of the calculations are shown in Fig. 5. Comparison of these results with the correspondent results for the slow deformation shows that for the adiabatic (5a and 5b) and air-cooling regimes (5c and 5d) the initial deformation rate has no significant effect on the following vibrations because both 100 s and 1 s are the enough intervals of time to establish steady state.

For the water-cooling regimes (5f and 5h) the fast preliminary deformation accompanied by heating of the rod results in the vibrogram similar to the adiabatic one. In

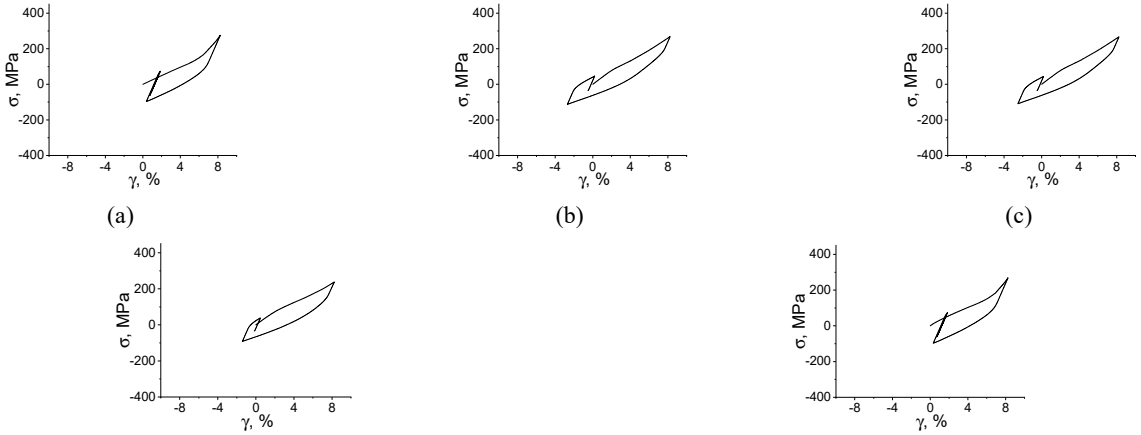

Fig. 6 Tangential stress – shear diagrams of the SMA element with the ambient temperature 330 K corresponding to (a) isothermal deformation; (b) adiabatic deformation; (c) heat exchange with $h_{conv} = 10$ W/(m^{2}K); (d) $h_{conv} = 500$ W/(m^{2}K); (e) $h_{conv} = 5000$ W/(m^{2}K)

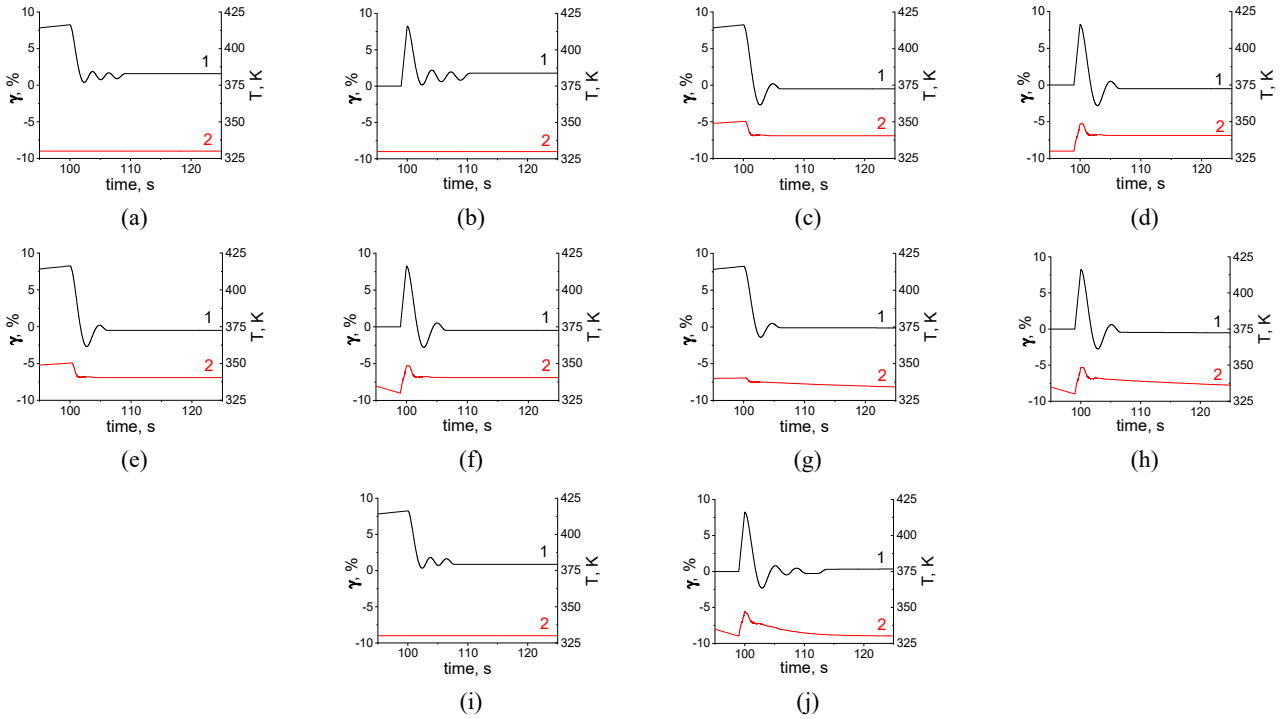

Fig. 7 Dependence of strain $\varepsilon(1)$ and temperature T(2) on time with the ambient temperature 330 K: (a) isothermal regime with slow initial deformation; (b) isothermal regime with fast initial deformation; (c) adiabatic regime with slow initial deformation; (d) adiabatic regime with fast initial deformation; (e) slow deformation with heat exchange $h_{conv} = 10$ W/(m^{2}K); (f) fast deformation with $h_{conv} = 10$ W/(m^{2}K); (g) slow deformation with $h_{conv} = 500$ W/(m^{2}K); (h) fast deformation with $h_{conv} = 500$ W/(m^{2}K); (i) slow deformation with $h_{conv} = 5000$ W/(m^{2}K); (j) fast deformation with $h_{conv} = 5000$ W/(m^{2}K)

contrast, the slow initial deformation (5e and 5g) gives enough time for the heat to come out so that the following reverse transformation leads to temperature decrease and better damping.

Tangential stress – shear diagrams at 330 K, at which the SMA rod is in the two-phase state and the phase yield limit is about 0 MPA, are shown in Fig. 6. Here one can see wide stress-strain loops in the first cycle of vibrations for all conditions of the heat exchange and correspondently good damping behavior of the pendulum (Fig. 7). The maximal number of free vibrations is 3 in the isothermal (7a and 7b) and forced water-cooling (7i and 7j) regimes when the temperature of the rod is either constant or changes insignificantly due to heating during the direct martensitic transformation. In all the other cases the vibrations decay in 1 – 2 cycles.

Since the heat exchange conditions and phase state of the SMA rod are of great importance for the decay rate, modeling of the control process with temperature variations was performed. Figures 8a and 8b illustrate strain and temperature variations in the austenitic (400 K) and martensitic (293 K) states of the SMA correspondently. Cooling from 400 K to 293 K leads to shortening of the vibration time from 55 s to 30 s for $h_{conv} = 500$ W/(m^2 K) (8c) and 10 s for $h_{conv} = 5000$ W/(m^2 K) (8d). Heating provokes the reverse martensitic transformation, making the damping properties of SMA worse. However, comparing the figures 8e and 8f one can see that when heating is technically inescapable, it is better when it takes more time. Heating from 293 K to 400 K during 10 s (8f) results in halving of the time interval of vibration while heating during 2 s (8e) leads to the strain-time dependence akin to that in the austenitic state (8a). At the same time, a very short heat impulse during a certain phase of vibration at temperature 293 K with water convection (8g) due to energy dissipation at martensitic transformations can cause effective vibration mitigation even compared to the pure martensitic state (8b).

4. Conclusions

Modeling of vibrations of systems containing SMA elements within the frames of the microstructural model was naturally extended to taking into account the latent heat of the martensitic transformation release and absorption during the direct and reverse martensitic transformation.

As the rotation pendulum usually works in some specific interval of frequencies depending on the SMA element length and diameter as well as on the parameters of the beam and the masses, there should be mentioned that the model can be easily generalized for other geometric sizes and shapes of working SMA elements. Although for quite accurate conclusions, it is necessary to solve the coupling thermal and mechanical problem, the approach under consideration allowed estimating the influence of the latent heat release/absorption and the heat exchange conditions on the vibrations of the rotation pendulum with the TiNi rod.

Numerical experiments showed that the rate of initial angular deviation of the pendulum from the equilibrium in the austenitic state affects the vibrations in the water-cooling regimes. Slow initial deformation, giving enough time for heat exchange with the outside, leads to a temperature decrease during the subsequent direct transformation and better damping.

As damping properties of martensite are better than that of austenite, the forced water-cooling regime is the most effective method of vibration damping, even although sometimes it is difficult to be implemented.

When it is technically impossible to avoid the reverse martensitic transformation in the SMA element, it is better to provide a low heating rate to mitigate the vibrations.

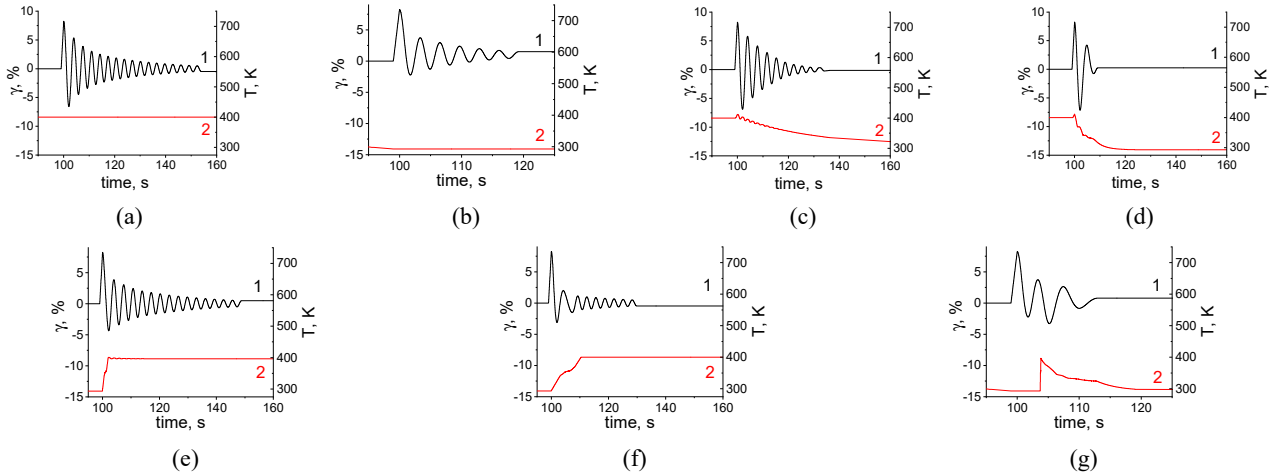

Fig. 8 Dependence of shear strain γ(1) and temperature T(2) on time for (a) isothermal vibration at 400 K; (b) isothermal vibration at 293 K; (c) cooling from 400 K to ambient temperature 293 K with $h_{conv} = 500$ W/(m^2 K) during vibration; (d) cooling from 400 K to ambient temperature 293 K with $h_{conv} = 5000$ W/(m^2 K) during vibration; (e) heating from 293 K to 400 K in 2 seconds during vibration; (f) heating from 293 K to 400 K in 10 seconds during vibration; (g) heating from 293 K to 400 K in 0.5 seconds with ambient temperature 293 K and $h_{conv} = 500$ W/(m^{2}K) during vibration

Acknowledgments

This work has been supported by the grant of the Russian Science Foundation, RSF 23-21-00167.

References

Armattoe, K.M., Bouby, C., Haboussi, M. and Ben Zineb, T. (2016), "Modeling of latent heat effects on phase transformation in shape memory alloy thin structures", *Int. J. Solids Struct.*, **88**, 283-295. https://doi.org/10.1016/j.ijsolstr.2016.02.024

Belyaev, S.P. and Volkov, A.E. (2001), "Control of vibrations in TiNi by periodic martensitic transformations", *J. Struct. Control*, **8**(2), 265-278. https://doi.org/10.1002/stc.4300080208

Belyaev, S.P., Volkov, A.E. and Voronkov, A.V. (1999), "Mechanical oscillations in TiNi under synchronized martensite transformations", *J. Eng. Mater. Technol.*, **121**(1) 105-107. https://doi.org/10.1115/1.2815990

Belyaev, S.P., Inochkina, I.V. and Volkov, A.E. (2003), "Modeling of vibration control, damping and isolation by shape memory alloy parts", *Proceedings of the 3rd World Conference on Structural Control* (*3WCSC*) (edited by F. Casciati), **2**, 779-789.

Belyaev, F.S., Evard, M.E., Ostropiko, E.S., Razov, A.I. and Volkov, A.E. (2019), "Aging effect on the one-way and two-way shape memory in TiNi-based alloys", *Shape Memory Superelast.*, **5**(3), 218-229. https://doi.org/10.1007/s40830-019-00226-5

Belyaev, F.S., Evard, M.E. and Volkov, A.E. (2022), "Effect of plastic deformation on the martensitic transformations in TiNi alloy", *Smart Struct. Syst., Int. J.*, **29**(2), 311-319. https://doi.org/10.12989/sss.2022.29.2.311

Boyd, J. and Lagoudas, A. (1996), "A thermodynamical constitutive model for shape memory materials. Part I. The monolithic shape memory alloy", *Int. J. Plast.*, **12**(6), 805-842. http://dx.doi.org/10.1016/S0749-6419(96)00030-7

Casciati, S. (2019), "SMA-based devices: insight across recent proposals toward civil engineering application", *Smart Struct. Syst., Int. J.*, **24**(1), 111-125. https://doi.org/10.12989/sss.2019.24.1.111

Casciati, F., Faravelli, L. and Petrini, L. (1998), "Energy Dissipation in Shape Memory Alloys", *Comput.-Aided Civil Infrastr. Eng.*, **13**(6), 433-442. http://doi.org/10.1111/0885-9507.00121

Evard, M.E. and Volkov, A.E. (1999), "Modeling of martensite accommodation effect on mechanical behavior of shape memory alloys", *J. Eng. Mater. Technol.*, **121**(1), 102-104. https://doi.org/10.1115/1.2815989

Gao, X., Huang, M. and Brinson, L.C. (2000), "A multivariant model for SMAs Part 1. Crystallographic issues for single crystal model", *Int. J. Plastic.*, **16**(10-11), 1345-1369. https://doi.org/10.1016/S0749-6419(00)00013-9

Graesser, E.J. and Cozzarelli, F.A. (1991), "Shape memory alloys as new materials for a seismic isolation", *J. Eng. Mech.*, **117**(11), 2590-2608. http://dx.doi.org/10.1061/(ASCE)0733-9399(1991)117:11(2590)

He, Y.J. and Sun, Q.P. (2010), "Frequency-dependent temperature evolution in NiTi shape memory alloy under cyclic loading", *Smart Mater. Struct.*, **19**(11), 115014. http://dx.doi.org/10.1088/0964-1726/19/11/115014

Helbert, G., Saint-Sulpice, L., Chirani, S.A., Dieng, L., Lecompte, T., Calloch, S. and Pilvin, P. (2017), "A uniaxial constitutive model for superelastic NiTi SMA including R-phase and martensite transformations and thermal effects", *Smart Mater. Struct.*, **26**(2), 025007. http://dx.doi.org/10.1088/1361-665X/aa5141

Helbert, G., Volkov, A., Evard, M., Dieng, L. and Chirani, S.A. (2020), "On the understanding of damping capacity in SMA: From the material thermomechanical behaviour to the structure response", *J. Intell. Mater. Syst. Struct.*, **32**(11), 1167-1184. https://doi.org/10.1177/1045389X20974453

Huang, M., Gao, X. and Brinson, L.C. (2000), "A multivariant micromechanical model for SMAs, Part 2. Polycrystal model", *Int. J. Plastic.*, **16**(10-11), 1371-1390. https://doi.org/10.1016/S0749-6419(00)00014-0

Jin, F., Zhao, C., Xu, P., Xue, J. and Lin, J. (2024), "Nonlinear vibration of SMA hybrid composite beams actuated by embedded pre-stretched SMA wires with tension-bending coupling effect", *J. Sound Vib.*, **568**, 117964. https://doi.org/10.1016/j.jsv.2023.117964

Kan, Q., Yu, C., Kang, G., Li, J. and Yan, W. (2016), "Experimental observations on rate-dependent cyclic deformation of super-elastic NiTi shape memory alloy", *Mech. Mater.*, **97**, 48-58. https://doi.org/10.1016/j.mechmat.2016.02.011

Kato, H. (2021), "Latent heat storage capacity of NiTi shape memory alloy", *J. Mater. Sci.*, **56**(13), 8243-8250. https://doi.org/10.1007/s10853-021-05777-6

Kaup, A., Altay, O. and Klinkel, S. (2021), "Strain amplitude effects on the seismic performance of dampers utilizing shape memory alloy wires", *Eng. Struct.*, **244**, 112708. https://doi.org/10.1016/j.engstruct.2021.112708

Khan, M.M., Lagoudas, D.C., Mayes, J.J. and Henderson, B.K. (2004), "Pseudoelastic sma spring elements for passive vibration isolation: Part I–modeling", *J. Intell. Mater. Syst. Struct.*, **15**(6), 415-441. https://doi.org/10.1177/1045389X04041529

Lagoudas, D.C., Khan, M.M., Mayes, J.J., Henderson, B.K. (2004), "Pseudoelastic SMA spring elements for passive vibration isolation: Part II–Simulations and experimental correlations", *J. Intell. Mater. Syst. Struct.*, **15**(6), 443-470. https://doi.org/10.1177/1045389X04041530

Leo, P.H., Shield, T.W. and Bruno, O.P. (1993), "Transient heat transfer effects on the pseudoelastic behavior of shape-memory wires", *Acta Metall. Mater.*, **41**(8), 2477-2485. https://doi.org/10.1016/0956-7151(93)90328-P

Liang, C. and Rogers, C.A. (1990), "One-dimensional thermomechanical constitutive relations for shape memory materials", *J. Intell. Mater. Syst. Struct.*, **1**(4), 207-234. https://doi.org/10.1177/1045389X9000100205

Likhachev, V.A. (1995), "Structure-analytical theory of martensitic unelasticity", *J. Phys. IV*, **05**(C8), 137-142. https://doi.org/10.1051/jp4:1995816

Louia, F., Michaelis, N., Schütze, A., Seelecke, S. and Motzki, P. (2023), "A unified approach to thermo-mechano-caloric-characterization of elastocaloric materials", *J. Phys. Energy*, **5**(4), 045014. https://doi.org/10.1088/2515-7655/acfb39

Meisner, L.L and Sivokha, V.P. (2004), "The effect of applied stress on the shape memory behavior of TiNi-based alloys with different consequences of martensitic transformations", *Physica B: Condens. Matt.*, **344**, 93-98. https://doi.org/10.1016/j.physb.2003.08.128

McCormick, P., Liu, Y. and Miyazaki, S. (1993), "Intrinsic thermal-mechanical behaviour associated with the stress-induced martensitic transformation in NiTi", *Mater. Sci. Eng.: A*, **167**(1-2), 51-56. https://doi.org/10.1016/0921-5093(93)90336-D

Patoor, E., Eberhardt, A. and Berveiller, M. (1996), "Micromechanical modelling of superelasticity in shape memory alloys", *J. Phys. IV*, **06**(C1), 277-292. https://doi.org/10.1051/jp4:1996127

Pence, T.J. (1999), "Mathematical modeling of shape memory alloys", Manside Project. Workshop Proc., II, 45-57.

Pieczyska, E.A., Tobushi, H. and Kulasinski, K. (2013),

"Development of transformation bands in TiNi SMA for various stress and strain rates studied by a fast and sensitive infrared camera", *Smart Mater. Struct.*, **22**, 035007. http://dx.doi.org/10.1088/0964-1726/22/3/035007

Regany, D., Majós, F., Barrau, J., Rosell, J., Ibáñez, M., Fréchette, L.G. and Vilarrubí, M. (2022), "Design and test of shape memory alloy fins for self-adaptive liquid cooling device", *Appl. Thermal Eng.*, **206**, 118010. https://doi.org/10.1016/j.applthermaleng.2021.118010

Qiu, C., Gong, Z., Peng, C. and Li, H. (2020), "Seismic vibration control of an innovative self-centering damper using confined SMA core", *Smart Struct. Syst., Int. J.*, **25**(2), 241-254. https://doi.org/10.12989/sss.2020.25.2.241

Song, D., Kang, G., Yu, C., Kan, Q. and Zhang, C. (2019), "Torsional whole-life transformation ratchetting under pure-torsional and non-proportional multiaxial cyclic loadings of NiTi SMA at human-body temperature: Experimental observations and life-prediction model", *J. Mech. Behavior Biomed. Mater.*, **94**, 267-278. https://doi.org/10.1016/j.jmbbm.2019.03.010

Sun, Q.-P. and Lexcellent, C. (1996), "On the unified micromechanics constitutive description of one-way and two-way shape memory effects", *J. Phys. IV*, **06**(C1), 367-375. https://doi.org/10.1051/jp4:1996135

Tabrizikahou, A., Kuczma, M., Łasecka-Plura, M., Farsangi, E.N., Noori, M., Gardoni, P. and Li, S. (2022), "Application and modelling of Shape-Memory Alloys for structural vibration control: State-of-the-art review", *Constr. Build. Mater.*, **342**(B), 127975. https://doi.org/10.1016/j.conbuildmat.2022.127975

Tadesse, Y., Thayer, N. and Priya, S. (2010), "Tailoring the response time of shape memory alloy wires through active cooling and pre-stress", *J. Intell. Mater. Syst. Struct.*, **21**(1), 19-40. http://dx.doi.org/10.1177/1045389X09352814

Tanaka, K. and Iwasaki, R. (1985), "A phenomenological theory of transformation superplasticity", *Eng. Fract. Mech.*, **21**(4), 709-720. http://dx.doi.org/10.1016/0013-7944(85)90080-3

Tanaka, K., Nishimura, F., Hayashi, T., Tobushi, H. and Lexcellent, C. (1995), "Phenomenological analysis on subloops and cyclic behavior in shape memory alloys under mechanical and/or thermal loads", *Mech. Mater.*, **19**(4), 281-292. http://dx.doi.org/10.1016/0167-6636(94)00038-I

Tiwari, N.D., Gogoi, A., Hazra, B. and Wang, Q. (2021), "A shape memory alloy-tuned mass damper inerter system for passive control of linked-SDOF structural systems under seismic excitation", *J. Sound Vib.*, **494**, 115893. https://doi.org/10.1016/j.jsv.2020.115893

Torra, V., Isalgue, A., Lovey, F.C. and Sade, M. (2015), "Shape memory alloys as an effective tool to damp oscillations", *J. Therm. Anal. Calorim.*, **119**, 1475-1533. https://doi.org/10.1007/s10973-015-4405-7

Trochu, F. and Terriault, P. (1998), "Nonlinear modeling of hysteresis material laws by dual kriging and application", *Comput. Methods Appl. Mech. Eng.*, **151**, 545-558.

Volkov, A.E. and Casciati, F. (2001), "Simulation of dislocation and transformation plasticity in shape memory alloy polycrystals", *Shape memory alloys. Advances in modelling and applications*, (Auricchio, F., Faravelli, L., Magonette, G., Torra, V., Eds.), CIMNE, Barcelona, pp. 88-104.

Volkov, A.E., Evard, M.E., Vikulenkov, A.V. and Uspenskiy, E.S. (2013), "Simulation of vibration isolation by shape memory alloy springs using a microstructural model of shape memory alloy", *Mater. Sci. Forum*, Vol. 738, pp. 150-154. https://doi.org/10.4028/www.scientific.net/MSF.738-739.150

Volkov, A.E., Evard, M.E., Red'kina, K.V., Vikulenkov, A.V., Makarov, V.P., Moisheev, A.A., Markachev, N.A. and Uspenskiy, E.S. (2014), "Simulation of payload vibration protection by shape memory alloy parts", *J. Mater. Eng. Perform.*, **23**, 2719-2726. https://doi.org/10.1007/s11665-014-1084-7

Volkov, A.E., Belyaev, F.S., Evard, M.E. and Volkova, N.A. (2015), "Model of the evolution of deformation defects and irreversible strain at thermal cycling of stressed TiNi alloy specimen", In: *MATEC Web Conferences*, Vol. 33, p. 03013. https://doi.org/10.1051/matecconf/20153303013

Wang, Z., Hang, G., Li, J., Wang, Y. and Xiao, K. (2008), "A micro-robot fish with embedded SMA wire actuated flexible biomimetic fin", *Sensors Actuators A: Phys.*, **144**(2), 354-360. https://doi.org/10.1016/j.sna.2008.02.013

Wilde, K., Gardoni, P. and Fujino, Y. (2000), "Base isolation system with shape memory alloy device for elevated highway bridges", *Eng. Struct.* **22**(3), 222-229. http://dx.doi.org/10.1016/S0141-0296(98)00097-2

Yan, Z., Zhu, J.N., Borisov, E., Riemslag, T., Scott, S.P., Hermans, M., Jovanova, J. and Popovich, V. (2023), "Superelastic response and damping behavior of additively manufactured Nitinol architectured materials", *Addit. Manuf.*, **68**, 103505. https://doi.org/10.1016/j.addma.2023.103505

Yin, H., He, Y. and Sun, Q. (2014), "Effect of deformation frequency on temperature and stress oscillations in cyclic phase transition of NiTi shape memory alloy", *J. Mech. Phys. Solids*, **67**, 100-128. https://doi.org/10.1016/j.jmps.2014.01.013